

# Pushing Photons with Electrons: Observation of the Polariton Drag Effect

D. M. Myers,\* B. Ozden, J. Beaumariage, and D. W. Snoke  
*Department of Physics and Astronomy, University of Pittsburgh, Pittsburgh, PA 15260, USA*

L. N. Pfeiffer and K. West  
*Department of Electrical Engineering, Princeton University, Princeton, NJ 08544, USA*  
 (Dated: November 17, 2022)

We show the direct effect of free electrons colliding with polaritons, changing their momentum. The result of this interaction of the electrons with the polaritons is a change in the angle of emission of the photons from our cavity structure. Because the experiment is a photon-in, photon-out system, this is equivalent to optical beam steering of photons using a DC electrical current. The effect is asymmetric, significantly slowing down the polaritons when they move oppositely to the electrons, while the polaritons are only slightly accelerated by electrons moving in the same direction.

It has long been known that an electron can impart momentum to a photon through the scattering interaction shown in the diagram of Figure 1, which can occur even in vacuum. However, in vacuum, this process has extremely low probability. In condensed matter systems, this probability can be made enormously larger by the renormalization of the gap energy between the electron and hole states down to just an electron-volt or so. Apart from the intrinsic interest in demonstrating the effect, it may have application in steering the direction of light by a DC electrical current, with the angle of deflection directly proportional to the current. However, observation of this effect has remained elusive.

We report here observation of this drag effect in a semiconductor structure that has been designed to maximize the light-matter coupling, namely strong coupling of exciton-polaritons in a solid-state microcavity. The physics of exciton-polaritons has been widely explored in recent years, and is well summarized in recent reviews, many of which have focused on Bose-Einstein condensation of polaritons [1–4]. In the present work, we use a polariton condensate, but the effect is not fundamentally one that only occurs for a condensate; rather, the condensate produces a spectrally narrow emission that makes the polariton drag effect easy to observe. The structures we use also allow long-distance transport over hundreds of microns [5, 6], which allows good momentum resolution in our measurements.

Recent theoretical work taking into account the polaron effect on an exciton interacting with a Fermi sea [7, 8] has predicted that applied DC current will give a drag force on exciton-polarons, and that the effect will also be significant when the excitons are coupled to photons, as in an exciton-polariton system. However, the drag effect can be understood even apart from the polaron effect as a purely collisional exchange of momentum due to Coulombic collisions between electrons and the excitonic part of a polariton, as discussed, e.g., in Ref. [9] and references therein.

**Experiment.** Exciton-polaritons in the strong-coupling limit are made by placing layers of semiconduc-

tors at the antinodes of a planar optical cavity. In the semiconductor layers, photon absorption leads to excited states known as excitons, consisting of a hole in the valence band and an electron in the conduction band, which can then recombine into photons. If the  $Q$ -factor of the cavity is high enough, and the vertex coupling the photon and exciton states is strong enough, new eigenstates appear which are no longer purely photon or exciton, but a superposition of both. In other words, a photon in the cavity spends some fraction of its time as an excited electron-hole pair.

The sample used in this experiment consists of a  $3\lambda/2$  microcavity formed by two distributed Bragg reflectors (DBRs), grown by molecular beam epitaxy (MBE). The DBRs were both made of alternating layers of  $\text{Al}_{0.2}\text{Ga}_{0.8}\text{As}$  and AlAs, with 32 periods in the top DBR and 40 in the bottom. 4 quantum wells (QWs), made of 7 nm GaAs layers with AlAs barriers, were placed at each of the 3 antinodes of the cavity. This microcavity design is the same used in previous work [5, 6, 10–14]. Long wires ( $\approx 200 \mu\text{m} \times 20 \mu\text{m}$ ) were formed by etching away the top DBR, confining the polaritons within the wire and exposing the QWs.

To allow colinear motion of free electrons in the same medium, two NiAuGe contacts were then placed upon the QWs at the ends of the wire, allowing electrical in-

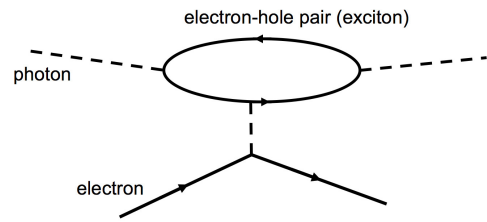


FIG. 1. The Feynman diagram for electron-hole-pair-mediated photon-electron interaction, where the dashed lines are photons and the solid lines are electrons.

jection into the QWs (see Figure 2). Hall measurements show that the wire regions are intrinsically  $n$ -doped of the order of  $10^{13} \text{ cm}^{-3}$ , and the contacts are  $n$ -type with heavy doping of the order of  $10^{19} \text{ cm}^{-3}$ . A continuous-wave (cw) stabilized M Squared Ti:sapphire pump laser was used to excite a spot on the wire, with a spot size of about  $20 \mu\text{m}$  FWHM, in the same arrangement used in Ref. 14. The pump was non-resonant, with an excess energy of about  $100 \text{ meV}$ , and mechanically chopped at  $400 \text{ Hz}$  with a pulse width of about  $60 \mu\text{s}$ . A source meter was used to sweep the applied voltage along the wires while measuring electrical current. The details of the fabrication and the electrical measurement are discussed in Ref. 13. The wire devices used in this study were all near resonance between the cavity and exciton modes ( $\delta = E_{\text{cav}} - E_{\text{exc}} = 0$ ).

Off-resonant optical pumping of this type of structure produces a cloud of excitons which then lose energy and fall down into polariton states. As in previous experiments with similar structures [11, 14], there are two critical thresholds for the optical excitation density. Above the lower threshold, a local quasicondensate is formed at the excitation spot, which can then ballistically expand away from the excitation region; above a higher critical threshold, the condensate jumps down dramatically into a much lower energy state, which is spectrally very narrow ( $< 0.1 \text{ meV}$  width at half maximum) and has high coherence length ( $\gg 200 \mu\text{m}$ ). We define the pump power needed to reach this second threshold as  $P_{\text{thres}}$ . The condensate is observed by recording the photons that leak out of the top mirror, using conventional imaging optics for both real-space (near field) and momentum-space (far field, Fourier plane) images, and a spectrometer for energy resolution. The leakage of photons out of the cavity is a tiny fraction of the population at any moment in time, because the  $Q$  of the cavity is very high ( $\sim 350,000$ ). The energy of the polariton condensate is determined by the external potential profile it feels, which is a combination of the single-particle polariton dispersion and the repulsion of polaritons from slow-moving excitons with much higher mass, and the density-dependent, repulsive polariton-polariton interaction, which tends to flatten any external potential felt by the polaritons.

**Experimental Results.** The experimental arrangement is shown in Figure 2(b), which gives the definitions of the axes directions and shows the voltage connections. Unless otherwise specified, the pump spot was located near the left ( $x = 0$ ) end of the wire for all of the data shown in this work. Figure 3 shows the polariton distribution along the wire at two different pump powers above threshold and at zero applied voltage. The energy “hill” near  $40 \mu\text{m}$  is due to the large population of reservoir excitons at the pump spot, which repulsively interact with the polaritons. The dips at the ends of the wire are due to the increased strain from the etching, similar to the

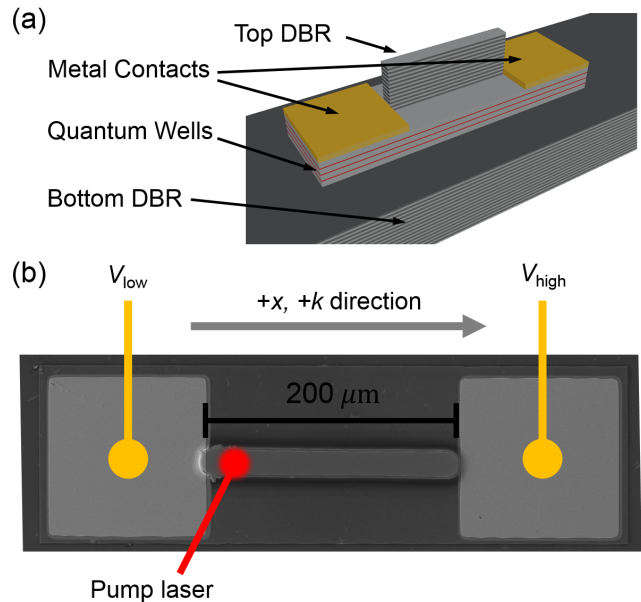


FIG. 2. (a) The etched microcavity structure with the Ni-AuGe contacts at each end of the wire. (b) Scanning electron microscope (SEM) image of a representative etched wire, with an overlay showing the experimental arrangement. The voltage connections of the source were connected to the device as shown. Thus, positive conventional current flowed in the direction of  $-x$ .

corners of the square pillars discussed in Ref. 11. A shallow cavity gradient along the  $+x$ -direction caused a small slope in the potential, with a total energy drop of about  $0.5 \text{ meV}$  across the wire. At the lower power, a quasicondensate at the location of the pump is clearly visible at high energy, as well as a significant population in the left-side end trap and a smaller population in the right-side trap. In the level region on the side away from the pump, a large mono-energetic condensate forms, filling a region of the wire about  $100 \mu\text{m}$  long. At higher power, the right-side end trap population becomes large enough to blue-shift itself to the same energy as the level region, forming a single mono-energetic condensate on the right side.

Figure 4 shows the energy and in-plane momentum ( $k_{\parallel}$ ) distribution of the polaritons at two different applied voltages. A population near  $k_{\parallel} = 0$  and at slightly lower energy is visible, and is emitted from the end trap. The larger population is from the level region of the wire, and clearly has an overall non-zero in-plane momentum, even with zero applied voltage. This is due to flow away from the pump spot, which is generally in the  $+x$ -direction. With applied negative voltage (Figure 4(b)), the overall momentum is clearly reduced. This voltage corresponds to conventional current flowing in the  $+x$ -direction, and thus electron current flowing in the  $-x$ -direction, which opposes the polariton flow. This clearly shows an effect

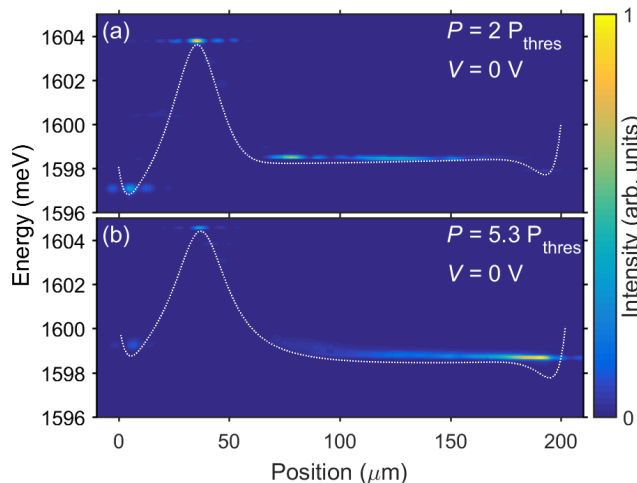


FIG. 3. PL intensity vs. energy and position along the length of the wire at zero applied voltage. The white dotted lines give the outline of the potential felt by the polaritons. The threshold power ( $P_{\text{thres}}$ ) was about 114 mW, and the powers used were (a)  $2P_{\text{thres}}$  and (b)  $5.3P_{\text{thres}}$ . The PL intensity was normalized separately for each image.

of drag upon the polaritons from the electrical current. When the wire is pumped on the other end, the overall effect is reversed, with the polaritons moving with momentum in the opposite direction. However, because the gradient of the cavity is in the opposite direction relative to the flow away from the pump in that case, the overall drag effect is reduced (see the Supplemental Information for further data and discussion).

Figure 5(a) shows the polariton distribution vs.  $k_{\parallel}$  for multiple applied voltages, and Figures 5(b) and (c) show the average  $k_{\parallel}$ , from plots similar to and including Figure 5(a), vs. current and applied voltage, respectively. A clear shift in the distribution is toward lower  $k_{\parallel}$  is visible with applied negative voltage, indicating drag upon the polaritons. When the current direction is reversed, there is very little effect on the overall momentum with applied positive voltage. The simplest explanation for this is that the cross section for electron-polariton collisions is proportional to their relative momentum, so that electrons moving oppositely to the polaritons impart significant momentum, while electrons moving in the same direction as the polaritons impart much less momentum. Simple calculations indicate that the velocities of the electrons and polaritons are comparable. The polariton velocity is measured directly from their momentum;  $0.5 \mu\text{m}^{-1}$  corresponds to  $v = \hbar k/m = 6 \times 10^7$  cm/s. The electron velocity can be estimated from the mobility, which our measurements give as approximately  $100 \text{ cm}^2/\text{V}\cdot\text{s}$ . For a voltage drop of 1 V over  $100 \mu\text{m}$ , this gives electron velocities of the order of  $10^6$  cm/s. By comparison, the sound velocity of the polaritons is nominally of the order of  $v_p = \sqrt{U n/m}$ , which is  $4 \times 10^6$  cm/s for the expected

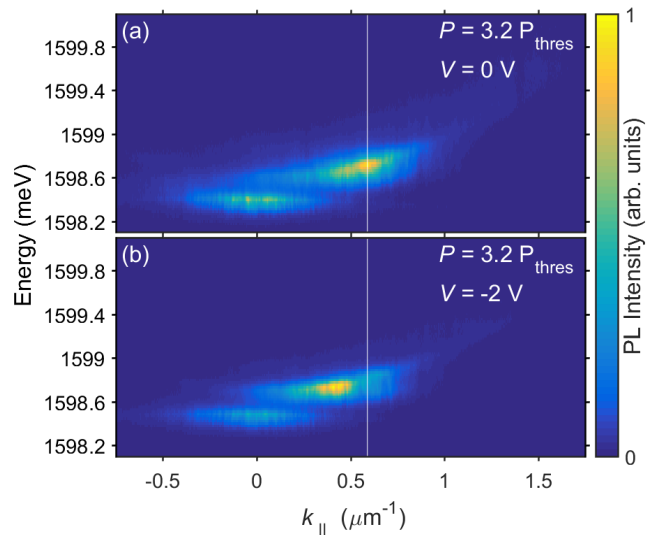


FIG. 4. PL intensity vs. energy and in-plane momentum ( $k_{\parallel}$ ). The threshold power ( $P_{\text{thres}}$ ) was about 114 mW, and the powers used were both about  $3.2P_{\text{thres}}$ . The applied voltage in each case (a) 0 V and (b) -2 V. The white vertical line is marking the  $k_{\parallel}$  value of the peak of the distribution at zero applied voltage to aid in comparing the two images. The PL intensity was normalized separately for each image.

polariton-polariton interaction strength of  $U \simeq 1 \mu\text{eV}\cdot\mu\text{m}^2$  [15, 16] for our multiple QW structure and our estimated density of the condensate of  $1/\mu\text{m}^2$ . This indicates that the average polariton velocity is higher than their sound velocity, so that they are not superfluid, and therefore their interactions with free electrons can be treated as single-particle scattering.

As seen in Figure 5(b), the saturation velocity for current in the direction co-moving with the polaritons increases with increasing density. One factor that contributes to this is that the gradient of the effective potential felt by the polaritons is greater for higher pump intensities, due to the larger exciton cloud potential. The density dependence of the velocity may also indicate that many-body effects come in to play. A model which accounts for ionization of the excitons to create free carriers, which then contribute to the drag effect as they respond to electric field, can reproduce some of the features of our data [17].

**Conclusions.** We have demonstrated proof of principle that a DC current can directly alter the momentum of photons moving in cavity; this has the direct effect of changing the angle of emission. In other words, this polariton drag effect is beam steering using a DC current to tune the angle of a light beam. As polariton structures move ever closer to practical room temperature devices [4], this basic effect may also be possible in those devices.

We also note that the propagation of a coherent polariton condensate for well over  $100 \mu\text{m}$  in this type of quantum wire allows the possibility of polariton circuits in

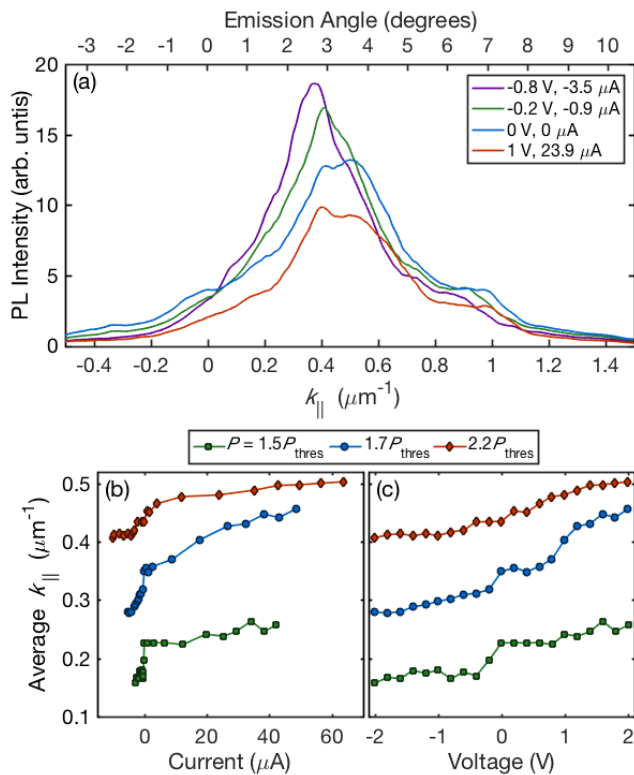


FIG. 5. (a) PL intensity vs.  $k_{\parallel}$  at various applied voltages, taken by integrating along the energy axis in images similar to Figure 4. These data are for a wire similar to that used for Figure 4, but with a threshold power of  $P_{\text{thres}} \approx 130$  mW. The power used in this case was  $2.2P_{\text{thres}}$ . (b) The average  $k_{\parallel}$  vs. current for various pump powers. (c) The average  $k_{\parallel}$  vs. applied voltage for various pump powers. The red diamonds in both (b) and (c) correspond to the same data used for (a).

which coherence is maintained over distances long enough for junctions, loops, and other elements. The long distance of coherent propagation is made possible by the long lifetime for photon leakage (high  $Q$ ) and low disorder of these samples, as well as the Bose condensation of the polaritons which causes the polaritons to flow to the global minimum of the entire structure.

**Acknowledgements.** The work at Pittsburgh was funded by the Army Research Office (W911NF-15-1-0466). The work of sample fabrication at Princeton was funded by the Gordon and Betty Moore Foundation (GBMF-4420) and by the National Science Foundation MRSEC program through the Princeton Center for Complex Materials (DMR-0819860).

\* dmm154@pitt.edu

[1] A. V. Kavokin, J. J. Baumberg, G. Malpuech, and F. P. Laussy, *Microcavities*, 2nd ed. (Oxford University Press, 2017).

- [2] I. Carusotto and C. Ciuti, *Rev. Mod. Phys.* **85**, 299 (2013).
- [3] H. Deng, H. Haug, and Y. Yamamoto, *Rev. Mod. Phys.* **82**, 1489 (2010).
- [4] D. W. Snoke and J. Keeling, *Physics Today* **70**, 54 (2017).
- [5] B. Nelsen, G. Liu, M. Steger, D. W. Snoke, R. Balili, K. West, and L. Pfeiffer, *Phys. Rev. X* **3**, 041015 (2013).
- [6] M. Steger, C. Gautham, D. W. Snoke, L. Pfeiffer, and K. West, *Optica* **2**, 1 (2015).
- [7] O. Cotlet, F. Pientka, R. Schmidt, G. Zarand, E. Demler, and A. Imamoglu, arXiv:1803.08509 (2018).
- [8] M. Sidler, P. Back, O. Cotlet, A. Srivastava, T. Fink, M. Kroner, E. Demler, and A. Imamoglu, *Nature Physics* **13**, 255 (2017).
- [9] V. Hartwell and D. W. Snoke, *Phys. Rev. B* **82**, 075307 (2010).
- [10] G. Liu, D. W. Snoke, A. Daley, L. N. Pfeiffer, and K. West, *Proceedings of the National Academy of Sciences* **112**, 2676 (2015).
- [11] D. M. Myers, J. K. Wuenschell, B. Ozden, J. Beaumariage, D. W. Snoke, L. Pfeiffer, and K. West, *Applied Physics Letters* **110**, 211104 (2017).
- [12] Y. Sun, Y. Yoon, M. Steger, G. Liu, L. N. Pfeiffer, K. West, D. W. Snoke, and K. A. Nelson, *Nature Physics* **13**, 870 (2017).
- [13] B. Ozden, D. M. Myers, M. Steger, K. West, L. Pfeiffer, and D. W. Snoke, in *Physics and Simulation of Optoelectronic Devices XXVI*, Vol. 10526 (International Society for Optics and Photonics, 2018) p. 105260H.
- [14] D. M. Myers, B. Ozden, M. Steger, E. Sedov, A. Kavokin, K. West, L. N. Pfeiffer, and D. W. Snoke, *Phys. Rev. B* **98**, 045301 (2018).
- [15] F. Tassone and Y. Yamamoto, *Phys. Rev. B* **59**, 10830 (1999).
- [16] P. M. Walker, D. V. Skryabin, A. Yulin, B. Royall, I. Farrer, D. A. Ritchie, M. S. Skolnick, and D. N. Krizhanovskii, *Nature Communications* **6**, 8317 (2015).
- [17] M. Glazov, I. Y. Chestnov, and A. Kavokin, private communication.

## Supplementary Information

### PUMPING ON THE HIGH-ENERGY END

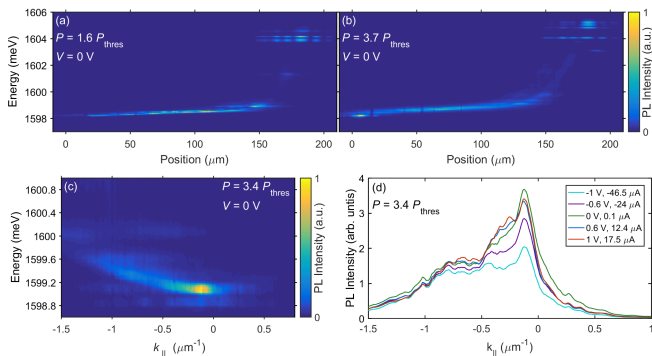


FIG. 6. (a) and (b) show PL intensity of the polaritons vs. energy and position along the length of the wire at zero applied voltage. The threshold power was about 150 mW under these conditions, and the powers used were (a)  $1.6P_{\text{thres}}$  and (b)  $3.7P_{\text{thres}}$ . (c) The PL intensity of the polaritons vs. energy and in-plane momentum ( $k_{\parallel}$ ) zero applied voltage. This image is from a different device from (a) and (b), so the energies are not directly comparable. However, the threshold power was similarly about 150 mW, and the power for the image shown was about  $3.4P_{\text{thres}}$ . (d) PL intensity integrated along the energy axis for data from the same device as (c) and under the same pump conditions.

In the main text, the data shown and discussed was for the specific case of pumping the wire on the low-energy end, with respect to the cavity gradient. In principle, the asymmetry in momentum can be flipped to the opposite direction by pumping on the opposite side. However, the gradient prevents a clean symmetric change of flow direction. Figure 6 shows a summary of the data when pumping on the high-energy end of the wire. In this case, since the polaritons flow downhill away from the pump, they do not form a mono-energetic condensate along the wire (Figure 6(a) and (b)). In the opposite case, with flow on a slight uphill away from the pump, the exciton reservoir helps to level the potential by filling the lowest energy end, and the polariton density is naturally higher near the source. This results in a level potential at relatively low densities. In this case, however, the reservoir actually makes the potential even less level, and the polaritons must flow all the way to the opposite end in order to form a level potential. The polaritons do clearly flow the  $\approx 175 \mu\text{m}$  to the far end and form a condensate, but there is no single condensate along the majority of the wire.

Figure 6(c) shows the momentum energy and momentum distribution under similar conditions. The flow is generally in the  $-x$ -direction as expected, but there is not a significant peaked population at large non-zero  $k_{\parallel}$ .

Comparing similar images at different applied voltages reveals no easily noticeable shift in momentum, unlike the case shown in the main text. However, a small effect is revealed by integrating along the energy axis (Figure 6(d)), which shows a small portion of the population between about  $-0.2$  and  $-0.4 \mu\text{m}^{-1}$  respond to applied voltage. This population shifts toward negative momentum with negative voltage and positive momentum with positive voltage, as expected from the more dramatic shifts shown in the main text. This effect is small, but the overall change in polariton flow from positive to negative in-plane momentum when changing the pump location confirms our claim that the overall momentum is largely due to flow from the pump spot.

### CURRENT-VOLTAGE CHARACTERISTICS

The current vs. voltage characteristics are similar to what was observed in the square pillar devices of Ref. 14, and can be seen in Figure 7. All data shown in the three separate axes are from the same device and pumped under similar conditions. An overall asymmetry is apparent when pumping on either end of the wire, and especially at lower powers. The asymmetry mostly disappears when pumping in the middle, indicating that it is due to the pump location. Furthermore, the asymmetry is nearly exactly opposite for pumping on opposite ends, which also indicates that it is primarily due to the pump spot location. We attribute this to greater illumination of the of the contact near the pump spot, creating free carriers that can carry current over the  $n-i$  band bending barrier, as discussed in Ref. 14.

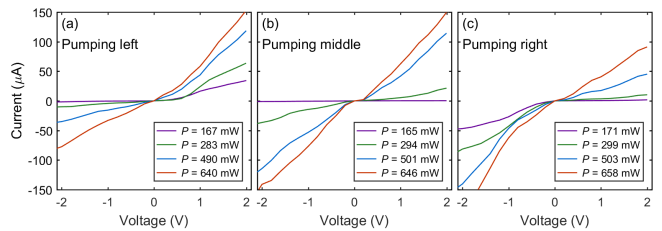


FIG. 7. Current vs. voltage for various pump powers and with different pump spot locations. The locations are given in the upper left of each plot, and are defined in reference to Figure 1(b) of the main text. Specifically, they are the (a) low energy end, (b) middle, and (c) high energy end of the wire, which correspond to the left, middle, and right sides of the  $x$ -axes used throughout this work. The approximate condensate threshold power for each case was (a) 130 mW, (b) 130 mW, and (c) 150 mW.

## MAXIMUM VELOCITY

As discussed in the main text, the application of positive voltage when pumping on the low energy end of the wire has little or no effect on the polariton momentum. We propose that this may be because the condensate has reached a maximum velocity simply from the flow away from the pump spot, so drag that would increase the velocity will have no effect on the velocity of the condensate. Following this reasoning, we plotted the average  $k_{\parallel}$  vs. the relative polariton density, shown in Figure 8. Since the distribution is strongly peaked in  $k_{\parallel}$ , and the shape is maintained overall as it shifts, the average  $k_{\parallel}$  is fairly representative of the maximum. The  $k_{\parallel}$  dependence on polariton density above threshold is very well fit by a power law which goes as  $n^{0.354}$ , where  $n$  is the polariton density. At very high densities the average momentum saturates. As discussed in the main text, the sound velocity of the polaritons increases as  $n^{0.5}$ . If many body effects are involved, such as a critical velocity of superfluidity, this is the natural unit of velocity for these effects. While the pump power has a direct influence on the expected sound velocity via an increase in density, changes in power also affect the potential felt by the polaritons. Higher powers result in a larger exciton cloud and thereby a larger force on the polaritons moving away from the pump, which also affects the overall velocity of

the polaritons.

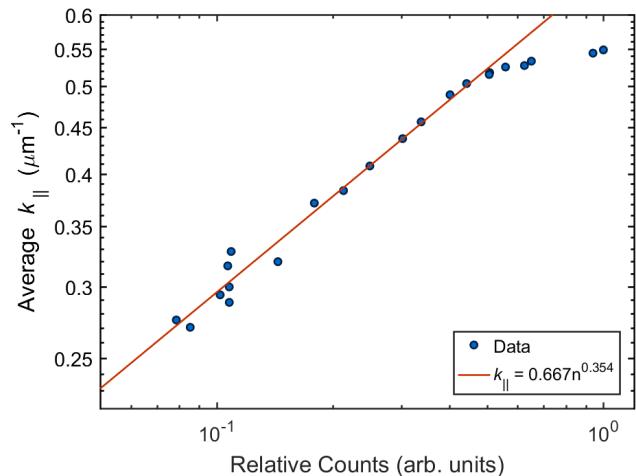


FIG. 8. Average  $k_{\parallel}$  vs. polariton counts, which is effectively the relative polariton density. The data come from averaging the energy-integrated curves similar to Figure 6(d) at many pump powers, but with the pump in the placement of the main text. The minimum pump power used was 200 mW, which is  $1.8P_{\text{thres}}$ . The data was fit using a power law, which is given in the figure legend.